Microstructured Collagen Films for 3D Corneal Stroma Modelling

Juha Prittinen (juha.prittinen@umu.se)
Umeå University
Xin Zhou
Umeå University
Ludvig Backman
Umeå University
Patrik Danielson
Umeå University

Research Article

Keywords: Microstructured, Corneal Stroma, perpendicular orientation

Posted Date: November 25th, 2020

DOI: https://doi.org/10.21203/rs.3.rs-111886/v1

Version of Record: A version of this preprint was published at Connective Tissue Research on December 12th, 2021. See the published version at https://doi.org/10.1080/03008207.2021.2007901.

Abstract

Corneal injury is a major cause for impaired vision around the globe. The fine structure of the corneal stroma plays a pivotal role in the phenotype and behaviour of the embedded cells during homeostasis and healing after trauma or infection. In order to study healing processes in the cornea, it is important to create culture systems that functionally mimic the natural environment as well as possible. In this study, we aimed to create a microstructured collagen film-based culture system that guides keratocytes (stromal cells) to their native, layerwise perpendicular orientation in 3D. By casting a micropattern (1,000 grooves/mm) on collagen vitrigels, we were able to make thin and transparent films that align cells along the grooves. The films provide an easily reproducible stroma model that maintains high cell viability and improves the preservation of the keratocyte phenotype in keratocytes that were subjected to fibroblast differentiation.

Introduction

The cornea is the outermost layer of the eye, playing a crucial role in light transmission. It is made out of five functionally distinct layers (epithelium, Bowman's membrane, stroma Descemet's membrane, and endothelium). As the majority of the cornea is comprised of the stroma, representing 90 % of the total thickness, it is a vital component for its optical clarity. The stroma's optical properties are mainly governed by the organisation of its structural components. [1] The stroma consists mostly of thin layers (2.5 µm) of aligned type I collagen fibres in an orthogonal conformation with sparse number of keratocytes. [2] There are other types of collagen present as well that help packing and maintaining the diameter of the type I fibres, such as type V collagen, which is the most prominent next to type I. [3] The stromal structure and its optical properties are also affected by a number of proteoglycans: Decorin, fibromodulin, lumican, and biglycan, all of which regulate type I collagen fibril formation through their leucine rich domain. [4-6]

Stromal wounds are common and if they heal with restored structure, they do not affect the vision. However, a dysregulated wound healing response may cause fibrotic scar formation and subsequent vision impairment, which is the 4th leading cause of blindness on an international scale. [7] Therefore, understanding the pathophysiological mechanisms for when and how the stroma repairs itself correctly is of clinical importance. Three different cell types can be found in the stroma during wound healing: Keratocytes, fibroblasts and myofibroblasts. It is known that soon after the wound is formed, the keratocytes at the edge of the wound change their phenotype to becoming fibroblasts. The fibroblasts then start remodelling the extracellular matrix around the wound by producing matrix metalloproteinases. [8] At the bed of the wound the fibroblasts begin to express α-smooth muscle actin (α-SMA) and change their phenotype to myofibroblasts. [9] Myofibroblasts are motile and contractile and therefore necessary for closing the wound gap. [10]

It is challenging to study the stromal cells in monolayer cultures, since it is not their typical environment. Especially the keratocyte phenotype readily drifts to a fibroblast-like one, when cultured in monolayers and in the presence of fetal bovine serum (FBS). [11] Several culture systems have been developed to remedy the shortcomings of monolayer cultures but more complicated culture systems are often based on materials that are not native to the cornea, such as silk and chitosan. [12-15] More recently, 3D bioprinting has been used for creating parts of the cornea, but at the moment it lacks the resolution to create cell guiding structures. [16,17] Collagen, being the major component of the stroma, has obvious benefits as a basis for a culture system and it has been shown to be a viable material for keratocyte maintenance even in the presence of FBS. [18,19] However, tuning the mechanical properties of collagen-based culture systems can be difficult, as the collagen concentration is often not sufficient to form mechanically robust systems [19]. Surface topography can be used to guide cell phenotype and morphology, and cell orientation can affect the orientation of the produced collagen. [20] It has also been shown that aligned collagen fibres can help transforming fibroblasts to keratocytes. [21] Collagen vitrification is a cost-effective way to create more robust structures and it has been used to create a corneal model before. [18] However, as far as we know, patterned collagen vitrigels for studying corneal stromal cells have not yet been explored. In this study, our aim was to create a multilayered and micropatterned collagen vitrigel-based culture system that would maintain and guide the corneal stromal cells to have a more natural organisation.

Results

Collagen film fabrication

Collagen vitrification and cross-linking yielded thin (19 ± 3 μm, average ± SD, n = 4) and clear films that ranged from 10% to 76% transparency across the visible spectrum (Fig. 1a, c). The casting of the pattern appeared to be uniform across the collagen surface when observed with SEM and the patterning did not affect the macroscopic appearance of the films (Fig. 1b). Collagen fibril diameter, as measured from the SEM micrographs, were approximately 82.6 ± 17.5 nm (average ± SD, n = 30).

Orientation and viability in 2D culture

Cell orientation was approximated by measuring the orientation of F-actin fibres. On the patterned surfaces 49% of the cells were aligned within ± 15° of an axis parallel to the groove direction while no preferential orientation could be discerned on the flat collagen or TCP surfaces (Fig. 2a and b). Since the grooved pattern could not be seen under light microscopy, SEM was done on patterned surfaces with cells on them to show the correlation between the pattern direction and cell orientation (Fig. 2c). The cell viability of keratocytes in 2D culture was equal between the collagen films and TCP after 7 days of culture (Fig. 2d).

Relative mRNA expression in 2D culture

mRNA expression was studied after three days of culture on all three culture surfaces: Patterned collagen film, flat collagen film, and TCP. During the culture, cells were either maintained as keratocytes or differentiated towards fibroblast or myofibroblast lineages as described in the methods section. [26-29] Expression of ALDH1 was significantly increased for keratocytes in the TCP group when compared to both flat and patterned collagen films (Fig. 3a). However, ALDH3 was significantly lower on TCP when compared to flat collagen film (Fig. 3a). Lumican, ALDH1, ALDH3, and α-SMA expressions for fibroblasts were significantly lower in the TCP group when compared to flat and patterned collagen films (Fig. 3b). Similarly, the lumican expression was significantly lower for myofibroblasts in the TCP group when compared to flat and patterned collagen films, but conversely ALDH1 was significantly higher in the TCP group in comparison to flat and patterned collagen films (Fig. 3c).

Protein expression

To assess the overall expression of relevant structural components, proteins were extracted for western blot analysis. Contrary to the mRNA expression levels, the quantity of α-SMA was higher for the myofibroblasts than for the keratocytes or fibroblasts. Furthermore, this difference could only be seen for cells cultured on the collagen films and not on TCP (Fig. 4a, b). The amount of produced lumican was comparable between all groups and culture conditions (Fig. 4a, c).

3D culture on stacked films

Patterned films were perpendicularly stacked inside a well-plate insert to create the 3D model. Even though the films were not deliberately attached to each other by any special mechanical or chemical means, they remained together when manipulated at the end of the experiment (Fig. 5a). Cell viability was assessed after four days of culture and approximately 86 ± 7 % (average ± SD, n = 5) of the cells were alive (Fig. 5b). Confocal microscopy of the films revealed that the cells retain their ability to orient themselves along the pattern even through a prolonged culture time of two weeks (Fig. 5c). The cell density at top, middle and bottom layers were measured to be approximately 65,000 ± 17,000, 47,000 ± 12,000, and 57,000 ± 4,000 (average ± SD; n = 5), respectively.

Discussion

In this work we created a novel collagen film-based scaffold for culturing and guiding keratocytes in 3D, mimicking the corneal stroma from a cellular perspective. Fabrication of a representative corneal model would help in studying the pathophysiological mechanisms of eye wound healing and scar formation in vitro. In the future, this kind of research could mitigate or prevent the loss of eyesight in patients with corneal injuries. So far, more effort has been focused in studies on the epithelium of the cornea and much less on the stroma, while often both are damaged. At the moment, major hurdles to overcome in creating a stroma model, are the anisotropy of the extracellular matrix and the correct induction of the repair phenotype of keratocytes. [31] There are many material alternatives to make viable tissue constructs, but as approximately 90% of the cornea is made up of collagen, it makes sense to use it as the basis of the

model. [15,32-34] So far, the methods used for the orthogonal orientation of collagen in the stromal lamellae are complicated and inaccessible to many researchers. [35,36] We believe that the model of our study adds to the existing 3D corneal in vitro models since it both consists of collagen and the cells are perpendicularly aligned in multilayers, similar to the in vivo condition.

Grated PET film was used to cast grooves on collagen films during vitrification, and after cross-linking the films were robust, flexible and easy to manipulate. The transparency of the films fell short of a native cornea and that of our previous silk-based mode, but still reached 33-90 % transparency of the native cornea. [37] This slightly lower transparency could, at least in part, be explained by the random orientation and low spacing between the collagen fibrils in the gel, in comparison to the collagen fibrils natively found in the corneal stroma. [26,38-40]

The manufacturer of the template film used for casting would not specify the groove dimensions due to imprecise manufacturing, but we could estimate from the SEM pictures the pitch to be less than 1 µm. While often micrometre-scale topographies are used for cell guidance by limiting the cells' ability to traverse ridges, [41] nanotopographies have been shown to be enough for cell orientation guidance through contact guidance. [42] The porosity of the surface may mitigate the contact guidance effect of the grooves, which at least in part may explain the wide spectrum of actin fibre orientations. It is also worth noting that cells can have a narrower distribution of orientations along the grooves than the actin fibres. [43] Nonetheless, the observations from the SEM micrographs and actin fibre orientation analyses support each other in that the grooved pattern leads to a good level of orientation along the grooves.

The collagen films did not affect the viability of keratocytes in either 2D or 3D cultures, and the cells populated the films thoroughly. It also appeared as if the morphology of the cells on the bottom layers had thin protrusions, reminiscent of keratocytes in vivo.

Keratocytes stay quiescent when cultured in serum-free conditions but they can be induced to proliferate when supplemented with FBS. However, the addition of FBS also drives the phenotype to a fibroblast lineage. It has been suggested that keratocytes can both proliferate and maintain phenotype in the presence of a relatively high concentration of FBS if they are cultured on collagen vitrigels. [44] This was also the case in our model, based on the fact that the lumican protein expression did not differ between the different FBS concentrations in the patterned collagen films, although the same phenomenon was seen in plain TCP culture conditions. It is known that keratocytes grown on flat surfaces have cortical F-actin organisation and lack stress fibres. [45] However, keratocytes cultured on microscale grooves can express stress fibres along the orientation of the grooves, appearing morphologically similar to fibroblasts while otherwise maintaining their keratocyte phenotype. [46,47] The gene expression data suggest that that the cells grown in 10 % FBS on the collagen films are more keratocyte-like than their counterparts grown on TCP, i.e. they express comparatively high amounts of lumican and ALDH [12]. This difference in expression cannot be seen on the cells grown in 2 % FBS, which could be due to the difference becoming evident only in higher concentrations of FBS. The myofibroblasts grown on the

collagen films appear to express a lower amount of keratocyte markers than their counterparts on TCP, which is further supported by the protein expression.

Our model harbours advantages in comparison to some other 3D models in the sense that it is based on collagen with multiple layers of cells perpendicularly arranged, similar to in vivo conditions. It could serve as a good model for studying corneal stromal wound healing. Since the epithelium in part does influence the repair phenotype of the keratocytes in a wound healing, addition of an epithelial layer would be needed for a more comprehensive model. With this model, adding layers to increase its complexity and similarity to a native cornea is feasible. Furthermore, the improved morphology of the keratocytes in the bottom layers of the 3D model may provide an interesting new path for exploring keratocyte phenotype maintenance.

Conclusions

A collagen film-based tissue model with a grooved topography was developed. The model supports stromal cells and guides the cell orientation in individual layers similarly to a native cornea while also maintaining a more keratocyte-like phenotype. Patterned collagen vitrigels have the potential to be a rapidly reproducible culture system that is highly accessible, not requiring specialized equipment. The realisation of this as a fully representative corneal model, however, requires the addition of other corneal elements.

Material And Methods

Cell source

Keratocytes were acquired from healthy corneal tissue through the Tissue Establishment, Eye Bank Umeå, at the University Hospital of Umeå. The tissues originated from diseased individuals that had chosen to be post-mortem tissue donors for research purposes according to the Swedish law. The Regional Ethical Review Board in Umeå has deemed the use of the tissue to be exempt from the requirement of approval from the board (2010-373-31M).

Cell culture

Keratocytes were isolated from the donated tissues as described previously. [22,23] Briefly, the corneal samples were received in DMEM supplemented with dextran, after which they were scraped with a scalpel to remove the remaining epithelial and endothelial cells. After this the tissues were rinsed with culture medium (DMEM/F-12, Gibco, Carlsbad, USA) and cut into pieces approximately 1-2 mm^2 in size and placed in a collagenase bath (2 mg/ml) at 37 °C overnight to free the keratocytes from the extracellular matrix. The following day, the digest was centrifuged to separate the cells before they were re-suspended in fresh medium supplemented with 2 % fetal bovine serum (FBS) (Gibco, Carlsbad, USA) and 1 % penicillin-streptomycin (Invitrogen, Carlsbad, USA). Keratocytes were differentiated into fibroblasts and myofibroblasts by adjusting the culture medium to include 10% FBS or 10 % FBS, 0,25 ng/ml TGF-B and

0,5 mM L-ascorbic acid 2-phosphate sesquimagnesium salt hydrate, respectively. [24,25] 20 000 cells/cm^2 were seeded on the films for all experiments. All cell cultures were maintained in a humidified incubator at 37 °C and 5 % CO_2. In this study, cells cultured in 2% FBS were referred to as keratocytes in accordance with findings in our previous studies. [22,23,26] Cells cultured in 10 % FBS were referred to as fibroblasts and cells cultured in 10 % FBS with TGF-B and ascorbic acid were referred to as myofibroblasts, in accordance with findings in other studies. [27-29]

Preparation of collagen surfaces

Optically grated polyethylene terephthalate films (1,000 grooves/mm, Edmund optics, York, UK) were cut into squares and cleaned with 70% ethanol. After drying, 12 µl/cm^2 of type I collagen solution (PureCol® EZ Gel 5 mg/ml, Advanced Biomatrix, San Diego, CA) was evenly spread on the grated films, either on the grated or flat side, and left in an oven to vitrify for 24 h at 37 °C. The following day 48 µl/cm^2 of the type I collagen solution was spread on top of the pre-existing collagen layer and left to vitrify for 24 h at 37 °C. The vitrified collagen films were cross-linked with 22.4 mM of N-(3-dimethylaminopropyl)-N'-ethylcarbodiimide hydrochloride (EDAC) and 4.6 mM of N-hydroxysulfosuccinimide sodium salt (sulfo-NHS) in 70% ethanol solution for 2 h at room temperature. After cross-linking, the collagen films were washed twice with 70% ethanol and then twice with phosphate-buffered saline (PBS). The films were prepared for cell culture by cutting them with a biopsy punch (⌀ = 8 mm) and sterilizing them under a UV light for 20 minutes.

Scanning electron microscopy

After the cells were maintained for three days on the collagen films, the films were fixed with 2.5% glutaraldehyde in sodium cacodylate buffer for 2.5 h at room temperature, washed in sodium cacodylate buffer and subsequently dehydrated in an increasing ethanol gradient, critical point dried and coated with 5 nm platinum. The morphology of the samples was analysed by field-emission scanning electron microscopy (SEM) (Merlin, Carl Zeiss, Oberkochen, DE) using in-lens secondary electron detector at accelerating voltage of 4 kV and probe current of 120 pA. Image analysis was done with Fiji. [30]

Immunocytochemistry

The cell orientation was measured from cells that had been grown on non-stacked films. Only cells that were maintained in 2% FBS were used for the measurement. After maintaining the cell cultures for seven days, the films were washed with PBS and the cells were then permeabilized in 0.3% Triton-X-100. The cells were then stained for F-actin (BODIPY FL Phallacidin, Life Technologies, Carlsbad, USA) according to the manufacturer's instructions. The cells were imaged using a fluorescence microscope (IX71, Olympus, Tokyo, JP). Cell morphology was visualized on stacked films. F-actin staining was used to visualize the cell morphology and it was performed as previously mentioned. All samples were mounted with ProLong Diamond Antifade Mountant with DAPI (4',6-diamidino-2-phenylindole, Life Technologies,

Carlsbad, CA). All stacked film constructs were imaged with a confocal microscope (SP8, Leica, Wetzlar, DE).

Cell alignment measurement

The cell orientation was estimated by calculating the orientation of the actin fibres in relation to the groove direction on the collagen film. The orientation of the actin fibres was calculated using OrientationJ Distribution plugin in ImageJ. Minimum coherency and energy were set to 5 % and the Gaussian window was approximated from the thickness of the fibres. The orientation was measured from two pictures per sample, which were then summed together and binned into 10 degree groups, i.e. orientation within a 10 degree window were clustered to one group. Measurements were normalized so that 0 degrees was the groove direction and the groove direction was determined by marking the edge of the films in the direction of the grooves prior to starting the experiment.

Gene expression analysis

Total RNA was isolated from the cells grown either on tissue culture polystyrene (TCP) or on the collagen films with or without patterning ($n \geq 5$) using RNeasy Mini kit (Qiagen, Hilden, DE). The isolation was done according to manufacturer's instructions for isolation from cell culture. 500 ng of the RNA was reverse transcribed to cDNA with High-Capacity cDNA Reverse Transcription Kit (Life Technologies, Carlsbad, USA). Gene expression was analysed from the cDNA with TaqMan Gene Expression Assays (Applied Biosystems, Carlsbad, USA). The gene expression is represented as relative expression of target gene, which is normalised to the expression on the patterned collagen films. β-actin was used as the endogenous control in all experiments. All probes were acquired from Applied Biosystems (Carlsbad, USA) and they are summarised in table 1.

Western blot

Cells were collected in triplicates and combined into one sample for each condition. Samples were lysed in Radioimmunoprecipitation Assay (RIPA) lysis buffer, supplemented with protease inhibitor (Sigma, St. Louis, MO) and diluted in Laemmli buffer (Bio-Rad, Hercules, USA) supplemented with β-mercaptoethanol. After boiling the samples, equal amounts of total protein were loaded into each well of a pre-made 12% gel (Mini-PROTEAN TGX, Bio-Rad, Hercules, USA) and ran at 120V for approximately 1 h. Subsequently, proteins were transferred to a polyvinylidene fluoride transfer membrane (Santa Cruz, Dallas, USA) for 60 min at 100 V. Membranes were blocked for 1 h in room temperature before primary antibody was added and incubated at 4 °C overnight. After washing, the membranes were exposed to the secondary antibody (conjugated with horseradish peroxidase, HRP) for 1 h and then to the enhanced chemiluminescence solution (GE healthcare, Little Chalfont, UK) for 5 min in room temperature. The membranes were developed using Odyssey Fc imaging system (LI-COR, Lincoln, USA) (supplementary Fig. S1). All antibodies used are summarized in Table 2.

Transparency

The collagen films were cut to fit in five wells of a 96 well plate. The films were submerged in PBS and the absorbance was measured at a physiologically relevant range of 300 to 700 nm using Synergy HT plate reader (BioTek, Winooski, USA). The absorbance was converted to transparency using equation (1).

$$(1)\ \%\text{transmittance} = 10^{-\text{absorbance}} \times 100$$

3D corneal model

Cells were seeded on the prepared collagen films and left to attach for 24 h before stacking three films with cells on top of each other into a cell culture insert (product# 353097, Falcon, New York, USA). One film without any cells was placed on top (Fig. 5a). A cylindrical weight was placed on top of the constructs to hold the films in place while cell culture media was added. All experiments with the 3D constructs were conducted with 2% FBS. The constructs were maintained for four days to determine cell viability with a live/dead assay (L-3224 Invitrogen, Carlsbad, USA) and for two weeks for collagen production and morphology analysis in a humidified incubator at 37 °C and 5 % CO_2. Cell morphology was studied by staining for actin fibres as described in the immunocytochemistry section. The cells were imaged with a confocal microscope (Leica SP8, Wetzlar, DE).

Cell viability

Metabolic activity of the keratocytes cultured on a single layer of the prepared films was analysed with CellTiter 96 AQueous One Solution Cell Proliferation Assay (Promega, Fitchburg, USA). The absorbance of the culture media was read at 490 nm with a Synergy HT plate reader (BioTek, Winooski, USA). Live/dead assay was performed according to manufacturer's instructions apart from increasing the incubation time from 30 minutes to 45 minutes to achieve stronger staining between the films.

Statistics

Statistical analysis was performed with one-way ANOVA and Tukey's multiple comparison post hoc test in all experiments. P-values below 0.05 were considered statistically significant. All experiments were performed in at least technical triplicates and successfully repeated at least three times, meaning at least three separate experiments were performed with cells isolated from different patients.

Declarations

Acknowledgements

The authors thank Assoc. Prof. Paul Kingham for facilitating our fluorescence light microscopy needs. We acknowledge the Biochemical Imaging Center at Umeå University and the National Microscopy Infrastructure, NMI (VR-RFI 2016-00968) for providing assistance in microscopy. The authors also thank Dr Maria Brohlin, Dr Mona Lindström, Ms Randi Elstad and Dr Berit Byström for help in providing the donated corneas from the biobank.

Author contributions

J.P., X.Z., L.B. and P.D. contributed to the study design and methodology. J.P and X.Z contributed to the experiments and data analysis. J.P. drafted the article. P.D. contributed to the resources. X.Z, L.B. and P.D. reviewed and edited the article. P.D. contributed to the acquisition of funding.

Additional information

The authors do not declare any potential conflicts of interest regarding the research, authorship or publication of this article.

References

1 Meek, K. M. & Knupp, C. Corneal structure and transparency. *Prog. Retin. Eye Res.***49**, 1-16, doi:10.1016/j.preteyeres.2015.07.001 (2015).

2 Chen, S., Mienaltowski, M. J. & Birk, D. E. Regulation of corneal stroma extracellular matrix assembly. *Exp. Eye Re.s***133**, 69-80, doi:10.1016/j.exer.2014.08.001 (2015).

3 Svensson, L. *et al.* Fibromodulin-null Mice Have Abnormal Collagen Fibrils, Tissue Organization, and Altered Lumican Deposition in Tendon. *J. Biol. Chem.***274**, 9636-9647, doi:10.1074/jbc.274.14.9636 (1999).

4 Dunlevy, J. R., Neame, P. J., Vergnes, J.-P. & Hassell, J. R. Identification of theN-Linked Oligosaccharide Sites in Chick Corneal Lumican and Keratocan That Receive Keratan Sulfate. *J. Biol. Chem.***273**, 9615-9621, doi:10.1074/jbc.273.16.9615 (1998).

5 Chen, S. & Birk, D. E. Focus on molecules: decorin. *Exp. Eye Res.***92**, 444-445, doi:10.1016/j.exer.2010.05.008 (2011).

6 Guo, C. & Kaufman, L. J. Flow and magnetic field induced collagen alignment. *Biomaterials***28**, 1105-1114, doi:10.1016/j.biomaterials.2006.10.010 (2007).

7 Fini, M. E. & Stramer, B. M. How the cornea heals: cornea-specific repair mechanisms affecting surgical outcomes. *Cornea***24**, S2-s11, doi:10.1097/01.ico.0000178743.06340.2c (2005).

8 West-Mays, J. A. & Dwivedi, D. J. The keratocyte: corneal stromal cell with variable repair phenotypes. *Int J. Biochem. Cell. Biol.***38**, 1625-1631, doi:10.1016/j.biocel.2006.03.010 (2006).

9 Chaurasia, S. S., Kaur, H., de Medeiros, F. W., Smith, S. D. & Wilson, S. E. Reprint of "Dynamics of the expression of intermediate filaments vimentin and desmin during myofibroblast differentiation after corneal injury". *Exp. Eye Res.***89**, 590-596, doi:10.1016/s0014-4835(09)00247-4 (2009).

10 Jester, J. V., Petroll, W. M., Barry, P. A. & Cavanagh, H. D. Expression of alpha-smooth muscle (alpha-SM) actin during corneal stromal wound healing. *Invest. Ophthalmol. Vis. Sci.***36**, 809-819 (1995).

11 Berryhill, B. L. *et al.* Partial restoration of the keratocyte phenotype to bovine keratocytes made fibroblastic by serum. *Invest. Ophthalmol. Vis. Sci.* **43**, 3416-3421 (2002).

12 Kumar, P., Pandit, A. & Zeugolis, D. I. Progress in Corneal Stromal Repair: From Tissue Grafts and Biomaterials to Modular Supramolecular Tissue-Like Assemblies. *Adv. Mater.***28**, 5381-5399, doi:10.1002/adma.201503986 (2016).

13 Ghezzi, C. E., Rnjak-Kovacina, J. & Kaplan, D. L. Corneal tissue engineering: recent advances and future perspectives. *Tissue. Eng. Part. B Rev.***21**, 278-287, doi:10.1089/ten.TEB.2014.0397 (2015).

14 Chen, J., Zhang, W., Kelk, P., Backman, L. J. & Danielson, P. Substance P and patterned silk biomaterial stimulate periodontal ligament stem cells to form corneal stroma in a bioengineered three-dimensional model. *Stem. Cell. Res. Ther.***8**, 260, doi:10.1186/s13287-017-0715-y (2017).

15 Gil, E. S. *et al.* Helicoidal multi-lamellar features of RGD-functionalized silk biomaterials for corneal tissue engineering. *Biomaterials***31**, 8953-8963, doi:10.1016/j.biomaterials.2010.08.017 (2010).

16 Isaacson, A., Swioklo, S. & Connon, C. J. 3D bioprinting of a corneal stroma equivalent. *Exp. Eye Res.***173**, 188-193, doi:10.1016/j.exer.2018.05.010 (2018).

17 Sorkio, A. *et al.* Human stem cell based corneal tissue mimicking structures using laser-assisted 3D bioprinting and functional bioinks. *Biomaterials***171**, 57-71, doi:10.1016/j.biomaterials.2018.04.034 (2018).

18 McIntosh Ambrose, W. *et al.* Collagen Vitrigel membranes for the in vitro reconstruction of separate corneal epithelial, stromal, and endothelial cell layers. *J. Biomed. Mater. Res. B Appl. Biomater.***90**, 818-831, doi:10.1002/jbm.b.31351 (2009).

19 Cui, Z. *et al.* Cell-laden and orthogonal-multilayer tissue-engineered corneal stroma induced by a mechanical collagen microenvironment and transplantation in a rabbit model. *Acta. Biomater.***75**, 183-199, doi:10.1016/j.actbio.2018.06.005 (2018).

20 Wang, J. H., Jia, F., Gilbert, T. W. & Woo, S. L. Cell orientation determines the alignment of cell-produced collagenous matrix. *J. Biomech.***36**, 97-102, doi:10.1016/s0021-9290(02)00233-6 (2003).

21 Muthusubramaniam, L. *et al.* Collagen fibril diameter and alignment promote the quiescent keratocyte phenotype. *J. Biomed. Mater. Res. A***100**, 613-621, doi:10.1002/jbm.a.33284 (2012).

22 Sloniecka, M. *et al.* Expression Profiles of Neuropeptides, Neurotransmitters, and Their Receptors in Human Keratocytes In Vitro and In Situ. *PLoS One***10**, e0134157, doi:10.1371/journal.pone.0134157 (2015).

23 Sloniecka, M., Le Roux, S., Zhou, Q. & Danielson, P. Substance P Enhances Keratocyte Migration and Neutrophil Recruitment through Interleukin-8. *Mol. Pharmacol.***89**, 215-225, doi:10.1124/mol.115.101014 (2016).

24 Karamichos, D. *et al.* TGF-beta3 stimulates stromal matrix assembly by human corneal keratocyte-like cells. *Invest. Ophthalmol. Vis. Sci.***54**, 6612-6619, doi:10.1167/iovs.13-12861 (2013).

25 Jester, J. V. *et al.* Myofibroblast Differentiation of Normal Human Keratocytes and hTERT, Extended-Life Human Corneal Fibroblasts. *Investig. Ophthalmol. Vis. Sci***44**, 1850-1858, doi:10.1167/iovs.02-0973 (2003).

26 Zhang, W., Chen, J., Backman, L. J., Malm, A. D. & Danielson, P. Surface Topography and Mechanical Strain Promote Keratocyte Phenotype and Extracellular Matrix Formation in a Biomimetic 3D Corneal Model. *Adv. Healthc. Mater.***6**, 1601238, doi:10.1002/adhm.201601238 (2017).

27 Jester, J. V. & Ho-Chang, J. Modulation of cultured corneal keratocyte phenotype by growth factors/cytokines control in vitro contractility and extracellular matrix contraction. *Exp. Eye Res.***77**, 581-592, doi:10.1016/s0014-4835(03)00188-x (2003).

28 Musselmann, K., Kane, B. P., Alexandrou, B. & Hassell, J. R. IGF-II is present in bovine corneal stroma and activates keratocytes to proliferate in vitro. *Exp. Eye Res.***86**, 506-511, doi:10.1016/j.exer.2007.12.004 (2008).

29 Sloniecka, M. & Danielson, P. Acetylcholine decreases formation of myofibroblasts and excessive extracellular matrix production in an in vitro human corneal fibrosis model. *J. Cell. Mol. Med.*, doi:10.1111/jcmm.15168 (2020).

30 Schindelin, J. *et al.* Fiji: an open-source platform for biological-image analysis. *Nat. Methods.***9**, 676-682, doi:doi:10.1038/nmeth.2019 (2012).

31 Myrna, K. E., Pot, S. A. & Murphy, C. J. Meet the corneal myofibroblast: the role of myofibroblast transformation in corneal wound healing and pathology. *Vet. Ophthalmol.***12 Suppl 1**, 25-27, doi:10.1111/j.1463-5224.2009.00742.x (2009).

32 Tonsomboon, K. & Oyen, M. L. Composite electrospun gelatin fiber-alginate gel scaffolds for mechanically robust tissue engineered cornea. *J. Mech. Behav. Biomed. Mater.***21**, 185-194, doi:10.1016/j.jmbbm.2013.03.001 (2013).

33 Wang, H. Y., Wei, R. H. & Zhao, S. Z. Evaluation of corneal cell growth on tissue engineering materials as artificial cornea scaffolds. *Int. J. Ophthalmol.***6**, 873-878, doi:10.3980/j.issn.2222-3959.2013.06.23 (2013).

34 Zimmermann, D. R., Fischer, R. W., Winterhalter, K. H., Witmer, R. & Vaughan, L. Comparative studies of collagens in normal and keratoconus corneas. *Exp. Eye Res.***46**, 431-442, doi:10.1016/s0014-

4835(88)80031-9 (1988).

35 Torbet, J. *et al.* Orthogonal scaffold of magnetically aligned collagen lamellae for corneal stroma reconstruction. *Biomaterials***28**, 4268-4276, doi:10.1016/j.biomaterials.2007.05.024 (2007).

36 Doughty, M. J., Seabert, W., Bergmanson, J. P. G. & Blocker, Y. A descriptive and quantitative study of the keratocytes of the corneal stroma of albino rabbits using transmission electron microscopy. *Tissue. Cell.***33**, 408-422, doi:DOI 10.1054/tice.2001.0195 (2001).

37 Boettner, E. A. & Wolter, J. R. Transmission of the Ocular Media. *Investig. Ophthalmol. Vis. Sci.***1**, 776-783 (1962).

38 Meek, K. M. & Knupp, C. Corneal structure and transparency. *Prog. Retin. Eye Res.***49**, 1-16, doi:10.1016/j.preteyeres.2015.07.001 (2015).

39 Freegard, T. J. The physical basis of transparency of the normal cornea. *Eye (Lond)***11 (Pt 4)**, 465-471, doi:10.1038/eye.1997.127 (1997).

40 Meek, K. M. Corneal collagen-its role in maintaining corneal shape and transparency. *Biophys. Rev.***1**, 83-93 (2009).

41 Martinez, E., Engel, E., Planell, J. A. & Samitier, J. Effects of artificial micro- and nano-structured surfaces on cell behaviour. *Ann. Anat.***191**, 126-135, doi:10.1016/j.aanat.2008.05.006 (2009).

42 Clark, P., Connolly, P., Curtis, A. S., Dow, J. A. & Wilkinson, C. D. Cell guidance by ultrafine topography in vitro. *J. Cell. Sci.***99 (Pt 1)**, 73-77 (1991).

43 Sales, A., Holle, A. W. & Kemkemer, R. Initial contact guidance during cell spreading is contractility-independent. *Soft. Matter.***13**, 5158-5167, doi:10.1039/c6sm02685k (2017).

44 Guo, Q. *et al.* Modulation of keratocyte phenotype by collagen fibril nanoarchitecture in membranes for corneal repair. *Biomaterials***34**, 9365-9372, doi:10.1016/j.biomaterials.2013.08.061 (2013).

45 Lakshman, N., Kim, A. & Petroll, W. M. Characterization of corneal keratocyte morphology and mechanical activity within 3-D collagen matrices. *Exp. Eye. Res.***90**, 350-359 (2010).

46 Jester, J. V. *et al.* Corneal keratocytes: in situ and in vitro organization of cytoskeletal contractile proteins. *Investig. Ophthalmol. Vis. Sci.***35**, 730-743 (1994).

47 Bhattacharjee, P., Cavanagh, B. L. & Ahearne, M. Effect of substrate topography on the regulation of human corneal stromal cells. *Colloids Surf. B.***190**, 110971, doi:https://doi.org/10.1016/j.colsurfb.2020.110971 (2020).

Tables

Table 1. Probes used for gene expression analysis from Applied Biosystems.

Gene name	Gene symbol	Assay ID
β-actin	ACTB	4352667
Lumican	LUM	Hs00929860_m1
Collagen V	COL5A1	Hs00609133_m1
Collagen III	COL3A1	Hs00943809_m1
Collagen I	COL1A1	Hs00164004_m1
Aldehyde dehydrogenase 3	ALDH3A1	Hs00964880_m1
Aldehyde dehydrogenase 1	ALDH1A1	Hs00946916_m1

Table 2. Antibodies used for immunofluorescence staining and western blot.

Antibody	Company	Code
Lumican	Abcam	168648
β-actin	Cell signaling	4967
α-SMA	Abcam	5694
Antirabbit IgG HRP-linked	Cell signaling	7074

Figures

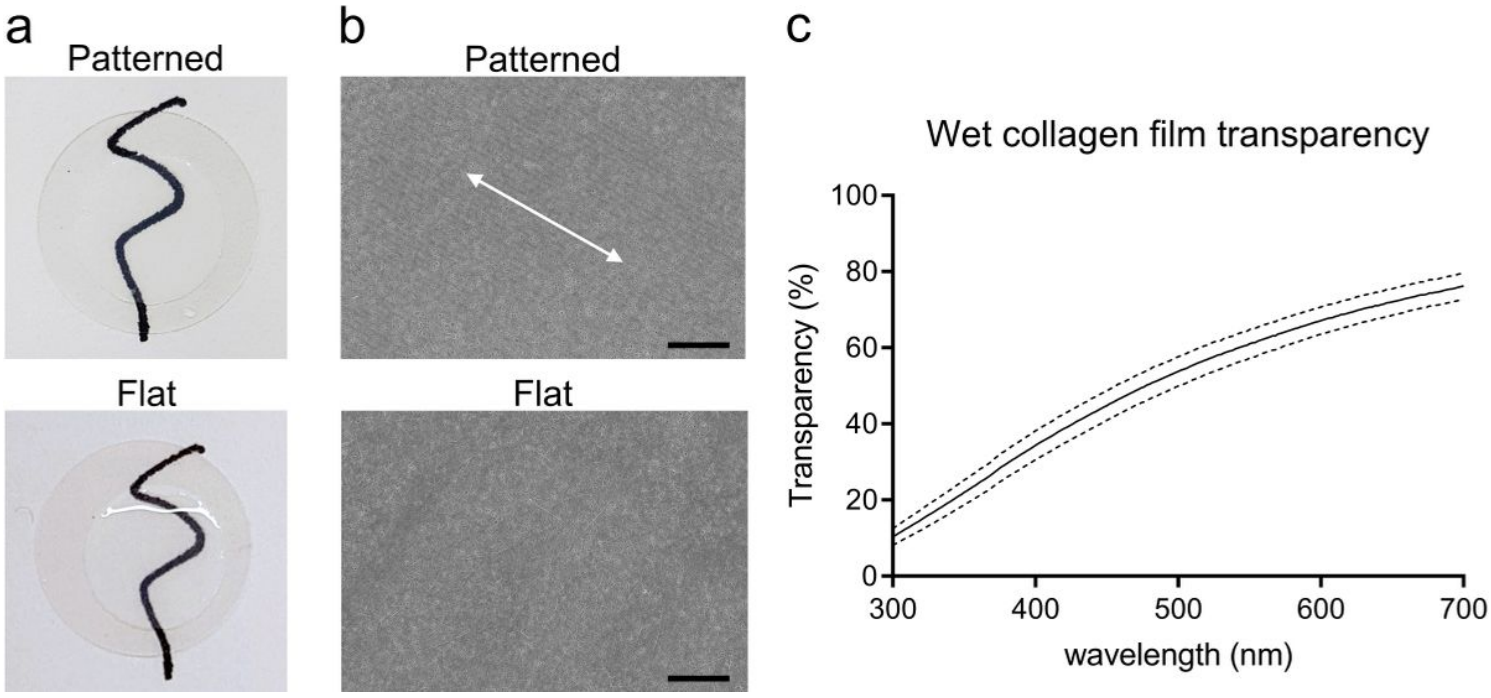

Figure 1

Characterisation of the collagen films. Under visual inspection the films were smooth and transparent when wetted, without any difference between the grooved and flat surfaces. Films were placed on glass coverslips for photography (a). Scanning electron microscopy of the patterned and flat collagen films. Arrow indicates the direction of the grooves SB = 10 μm (b). Mean patterned collagen film transparency across the visible light spectrum. SD is shown with the dashed line (c).

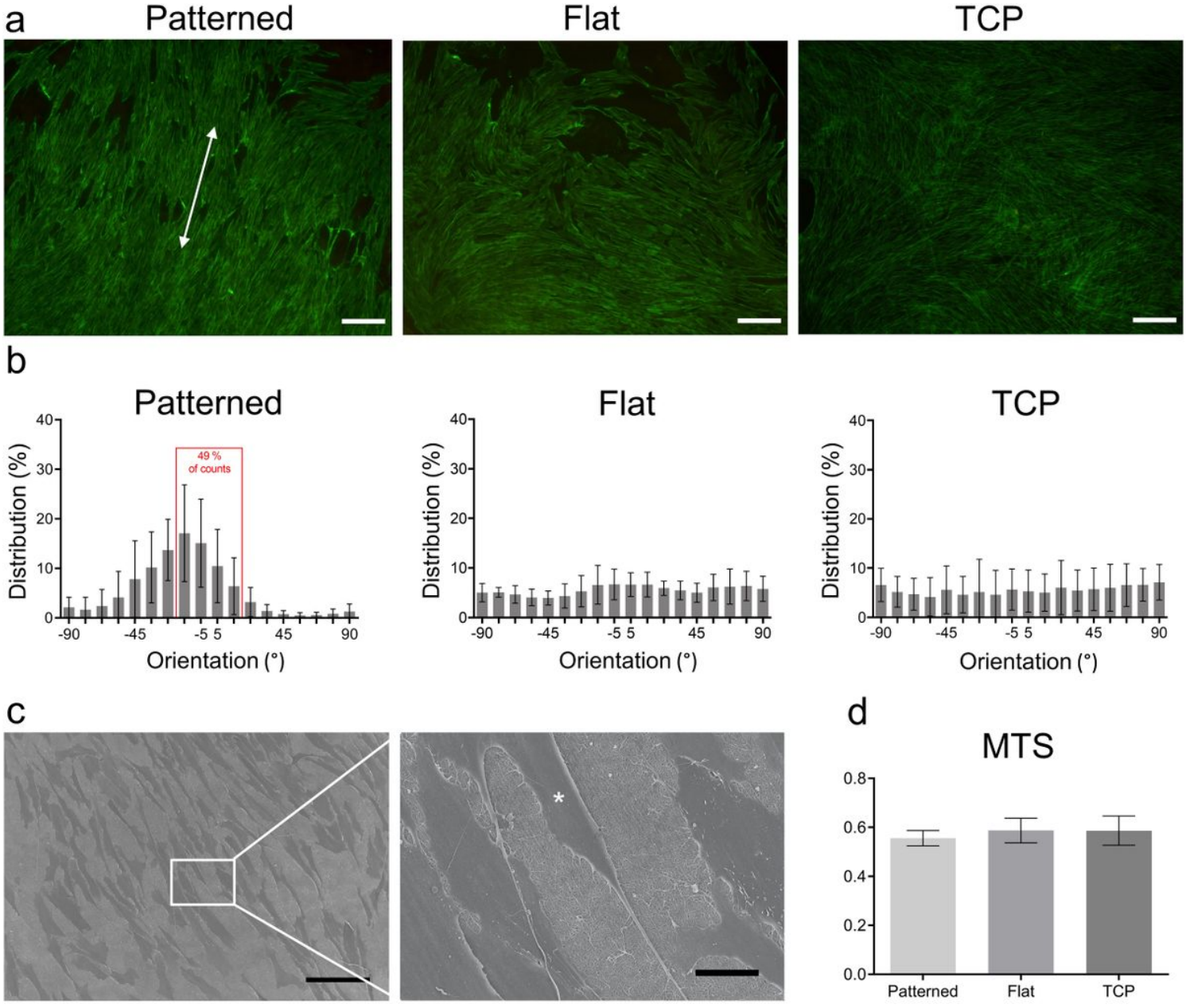

Figure 2

Cell orientation on the patterned films and cell viability. Actin staining of keratocytes cultured on patterned, flat and tissue culture polystyrene. SB = 100 μm (a). Distribution of mean actin fibre orientation angles after seven days of culture (b). Representative scanning electron micrograph of patterned collagen surface. Arrows indicate the orientation of the grooves and asterisk indicates a cell. SB = 100 μm (left)

and 15 µm (right) (c). MTS of patterned, flat and polystyrene after seven days of culture (d). Results are shown as average ± SD.

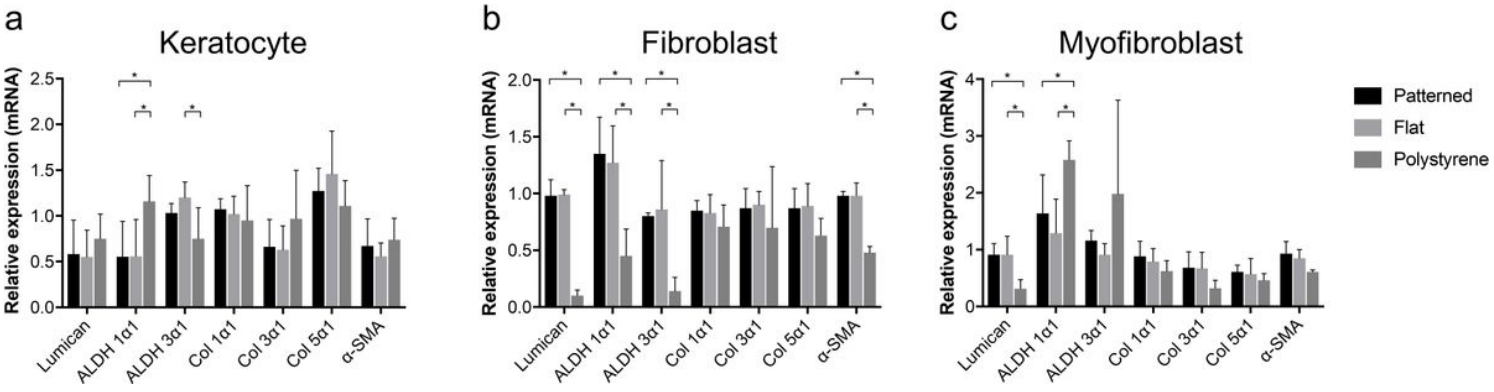

Figure 3

Relative mRNA expression of keratocyte markers. Relative mRNA expression in maintained keratocytes (a), keratocytes differentiated into fibroblasts (b), and keratocytes differentiated into myofibroblasts (c). The results are shown as average ± SD. * P < 0.05

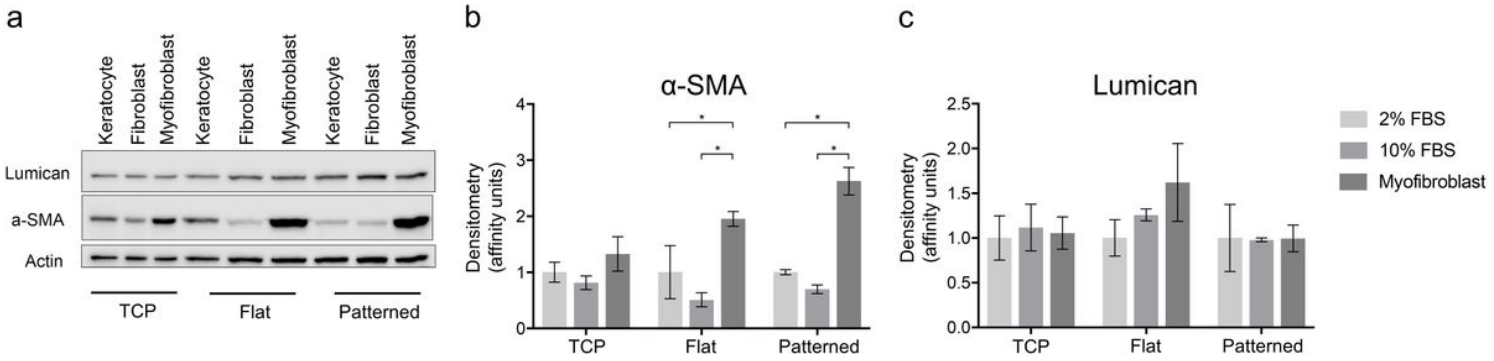

Figure 4

Protein expression of keratocyte markers. The expression levels of α-SMA and Lumican were normalised to Actin (a). α-SMA (b) and Lumican (c) expressions were compared between different phenotypes. The results are shown as average ± SD. * P < 0.05

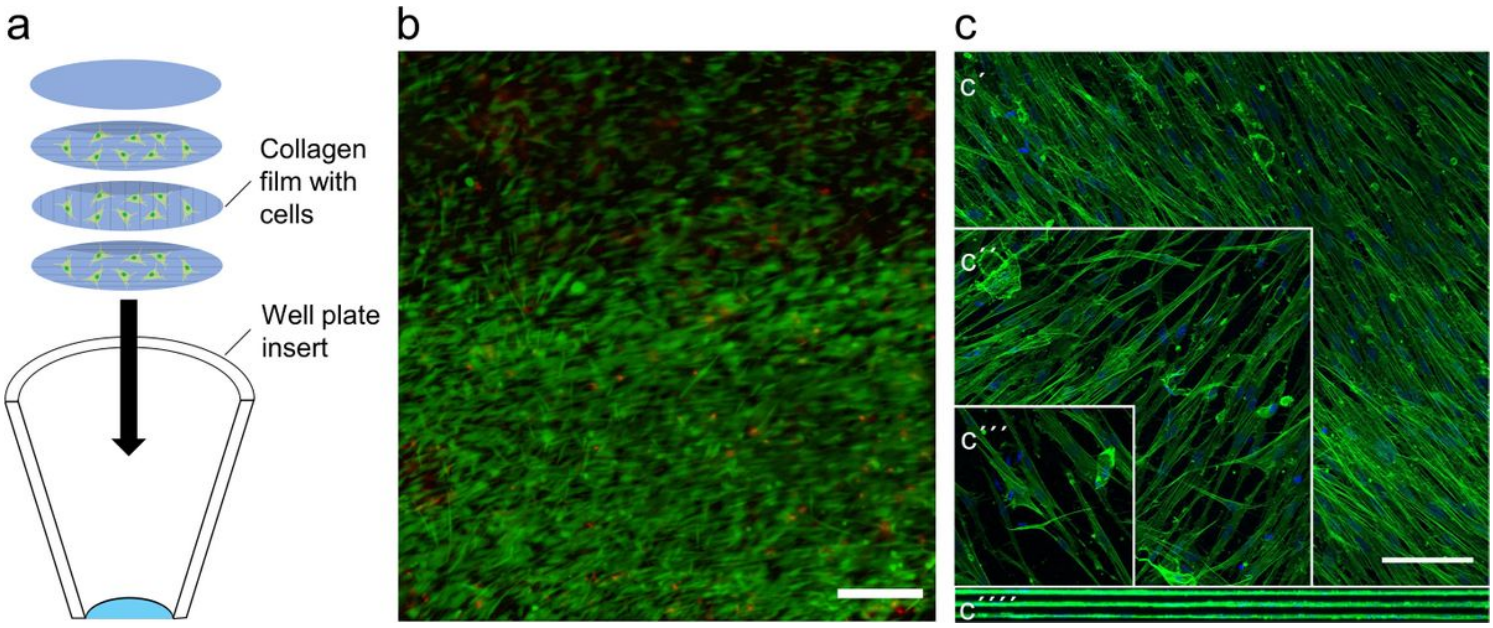

Figure 5

Representations of three-dimensional cell culture. Schematic representation of stacked films and the conical insert that they were maintained in (a). Representative image of live/dead cell viability assay, in which live cells are shown as green and dead cells as red. SB = 100 µm (b). Representation of individual layers stained for F-actin (green), where c´, c´´ and c´´´ are the top, middle and bottom layers, respectively. c´´´´ indicates the orthogonal projection of the stack. SB = 100 µm (c).

Supplementary Files

This is a list of supplementary files associated with this preprint. Click to download.

- Supplementalinformation.pdf